J. Sci. Trans. Environ. Technov. 2011, 5(1) :30- 36

Scientific Transactions
in Environment and
Technovation

Enhancement of desalination process for potable water productivity in a low cost spherical solar still with charcoal absorber

T. Arunkumar[1], R. Jayaprakash[1*], K. Perumal[1], Sanjay Kumar[2] and A.K. Abdul Hakeem[3]

[1]Department of Physics, Sri Ramakrishna Mission Vidyalaya College of Arts and Science, Coimbatore, Tamil Nadu, India.
[2]Department of Mathematics, Sri Ramakrishna Mission Vidyalaya College of Art and Science, Coimbatore, Tamil Nadu, India.
[1]Centre for Appropriate Management Chandragupt Institute of Management Chajubagh, Patna - 800 001, Bihar, India.

Abstract

A comparative study was made between the performance of desalination process in spherical solar still with and without charcoal absorber. It was studied in the climatic conditions of Coimbatore (11° N latitude), India. The area of the still was 0.30 m^2. The still was covered by low density polyethylene sheet of thickness 0.107 mm with 90% of transmittance. The absorbance of water level was further increased by floating charcoal at the surface of the water level. The internal heat transfer mode and external heat transfer mode were calculated for with and without charcoal absorber experiments. The efficiency of the still was calculated for both studies. Saturated vapor pressure (SVP) and latent heat evaporation were also calculated. The increase in potable water productivity caused, when using a spherical shape as well as adding charcoal was analyzed.

Keywords: desalination, external heat transfer, internal heat transfer, saturated vapour pressure, spherical solar still

INTRODUCTION

We can not able to separate the important word "water", from the environment. Because it is essential part of our life cycle. The world is polluted due to the increasing population and the needs of the human beings. So the whole environment is being collapsed at a rapid rate. About 97% of the world's water is salt water in the oceans, 3% of all fresh water is in ground water, lakes and rivers, which supplies the most that needed by the human and animals. So every human and animal depend on the ground water source and the rivers. But these sources are also getting polluted by the fast growing factories and chemical wastes. The world's water consumption rate is doubling every 20 years, increasing two times the rate of population growth. It is projected that by the year 2025, water demand will exceed supply by 56%, due to persistent regional droughts, shifting of the population to urban coastal cities, and industrial growth. The supply of fresh water is on the decreasing mode, whereas water demand for food, industry and people is on the rising mode. Lack of fresh water reduces economic development and lowers living standards. There is an important need for clean and pure drinking water in many developing countries. Often water sources are brackish (*i.e.* contain dissolved salts) and/or contain harmful bacteria, and hence cannot be used for drinking. In addition, there are many coastal locations where seawater is abundant but potable water is not available. Pure water is also used for batteries, hospitals and schools. Distillation is one of many processes that can be used for water purification. This requires an energy input like heat. Solar radiation can also be a source of energy in this process. In purification, water gets evaporated, and separated as water vapor from dissolved matter, which is condensed as pure water. The most common renewable energy sources are from solar desalination, wind, geothermal energy and ocean. At present, use of renewable energy sources for desalination is very limited. Out of world's total renewable energy sources extracted, renewable energy extracted through desalination is about 0.02% only. Desalination powered renewable energy sources can be an ideal solution for small scale communities, where affordable fossil fuel supply is not available (Rodriguez, 2004). A solar still is a device by which distilled or portable water can be produced from saline water sources such as sea water or brackish water. Solar stills are normally used to provide small scale portable water needed in remote isolated locations (Cappelletti, 2002). A review of various designs of solar stills was made by Malik *et al.,* (1982). The different designs of solar stills were studied by Badran and Al-Hayek (2004). Al-Hussaini and Smith used vacuum technology (1995). Kalogirou (1998) designed a parabolic trough solar stills and El-Sebaii developed triple basin solar stills (2005) for enhancing productivity from the solar stills. In order to improve the performance of conventional solar stills,

---

*Corresponding Author
email: *jprakash_jpr@rediffmail.com*

several other designs have been developed such as the double basin type (Al-Karaghouli and Alnaser 2004), multi basin type (Tiwari *et al.*, 1993), inverted trickle (Badron, 2001) and pyramid type (Kabeel, 2007).

The present work explains the performance of the spherical solar still using charcoal absorber. The performance of the newly designed spherical solar still is analyzed with and without charcoal absorber. The distilled water output is also compared between both studies. The internal and external heat transfer modes are calculated.

MATERIALS

Fig. 1shows the pictorial view of Spherical Solar Still. Fig. 2 shows the schematic diagram of 0.30 m^2 spherical solar still. The total height of the still is about 0.63 m. The still consists of circular basin of diameter 0.60 m which is made up of steel. The circular absorber basin is coated with black paint for maximum absorption of incident solar radiation. The circular basin is fixed at the middle of the spherical aluminum ring like a mesh at radial height of 0.28 m where saline water is stored. The storage capacity of the basin is around 16 litres. The basin in the spherical solar still is fitted without having any physical contact with the top cover made of low density polyethylene sheet. The low density polyethylene sheet of thickness 0.107 mm is spread over the spherical shaped ring like a mesh. A gap of 0.03 m is maintained between the circular basin and top cover. The outer cover of polyethylene is molded over the still without any air gap to prevent vapor leak. The evaporated water which is condensed over the top cover passes between this gap and creeps down towards the distilled water collection segment. The calibrated thermocouples are used to measure the temperature in the basin and also at different places of the still.

METHODS

Experimental measurements are performed to evaluate the performance of the spherical solar still under the clear climatic conditions of Coimbatore, India (11° N latitude). The basin is filled with 8 litres of water. A layer of charcoal was allowed to float on the surface of the water. The experiment was conducted between 9:00 AM to 5:00 PM and readings were recorded once in every 30 minutes. The water temperature, air temperature, inner cover temperature and outer cover temperature were recorded at regular intervals of time. As charcoal is acting as a good absorber on the surface, it rises the temperature of the water and so the productivity rate increases to an optimum level. The same study was repeated without charcoal absorber inside the spherical solar still. The water level in the basin rapidly decreased due to more evaporation of water in clear sunny days. So a water tank was connected to the still and water level was maintained at the same level for all studies. The distillated output of spherical solar still was frequently measured by a measuring jar at regular intervals. The measuring jar was placed at the outlet of the solar still.

HEAT TRANSFER COEFFICIENTS

Internal Heat Transfer Mode

Heat transfer inside the still was predicted by using the equation proposed by Malik *et al.*, (1974). Heat is transported inside the still by free convection of air. It releases its enthalpy upon air which is coming in contact with the glass cover. The heat transfer per unit area per unit time due to the convection is

$$Q_{ci} = h_{ci}(T_w - T_g)\ W/m^2 \qquad (1)$$

Where

$$h_{ci} = 0.884\ [(T_w - T_g) + [\ R_1\ (T_w - T_g)(T_w + 273)/268.9'\ 10^{-3} - R_2 - R_1(T_w + 273)]\ W/m^2 \qquad (2)$$

Heat transfer mode inside the still due to evaporation is given by

$$Q_{ei} = h_{ei}(T_w - T_g)\ W/m^2 \qquad (3)$$

Where

$$h_{ci} = \left(16.276 \times 10^{-3}\right)\ h_{cw}.R_1 \qquad (4)$$

Here R$_1$ and R$_2$ are evaluated by fitting the saturation vapor pressure data in the range of interest to a straight line.

$$Q_{ri} = h_{ri}\left(T_w - T_g\right) \mathrm{W/m^2} \qquad (5)$$

Where

$$h_{ri} = \varepsilon_w \varepsilon_{ch} \sigma \frac{\left(T_w + 273\right)^4 - \left(T_g + 273\right)^4}{\left(T_w - T_g\right)} W / m^2 \qquad (6)$$

Heat Transfer Rate outside the Still

Heat transfer per unit area per unit time outside the still is calculated using

$$Q_{ac} = h_{ca}(T_g - T_q) + e_g s\ [(T_g + 273)^4 - (T_{sky} + 273)^4]\ W/m2 \qquad (7)$$

Here h$_{ca}$ is a function of wind velocity and is given by Duffie and Beckman (1974) as

$$h_{ca} = 5.7 + 3.8V \qquad (8)$$

T$_{sky}$= (T$_a$-12) is the apparent sky temperature for long wave radiation.

The following is the empirical relation for free convection heat transfer from inside the sphere

$$Nu_f = \frac{hd}{k_f} = 2 + 0.392 Gr_f^{\frac{1}{4}} \qquad (9)$$
$$for 1 \le Gr_f \le 10$$

Fig.1. Pictorial view of Spherical Solar Still

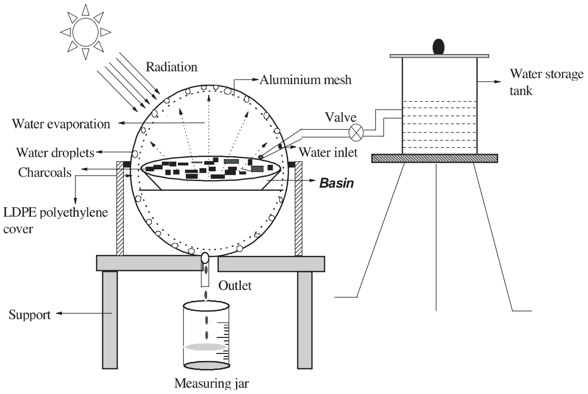

Fig. 2. Schematic view of a Spherical Solar Still

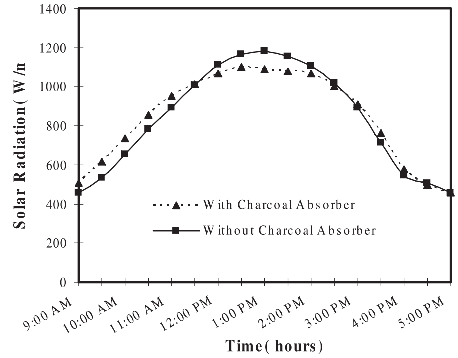

Fig . 3. Variation of solar radiation with respect to time

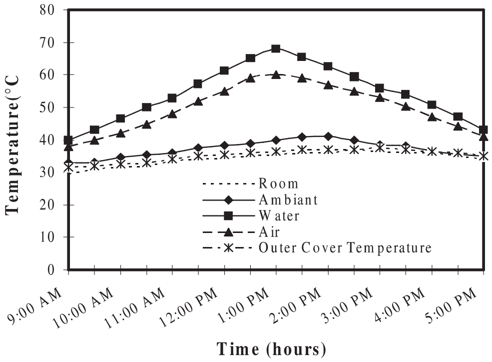

Fig. 4. Variation of temperature with respect to time for still with charcoal absorber

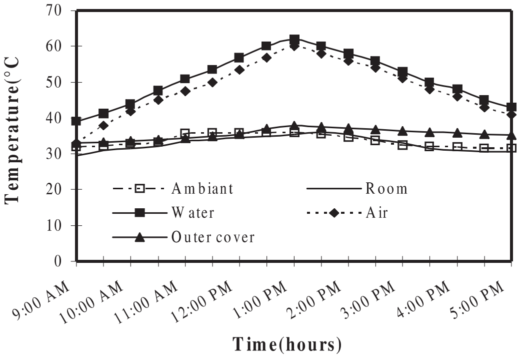

Fig.5. Variation of temperature with respect to time for still without charcoal

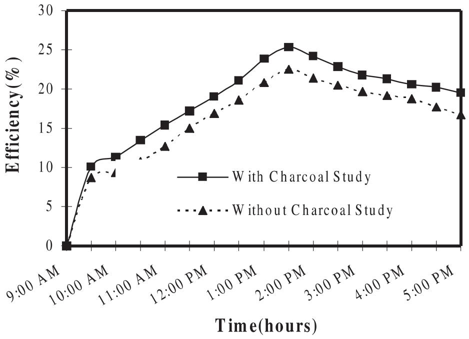

Fig.6. Variation of efficiency with respect to time

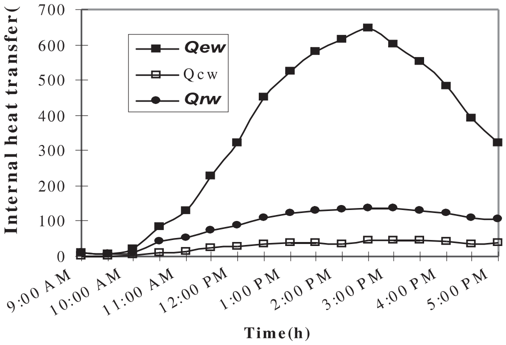

Fig. 7. Variation of internal heat transfer for without charcoal performance

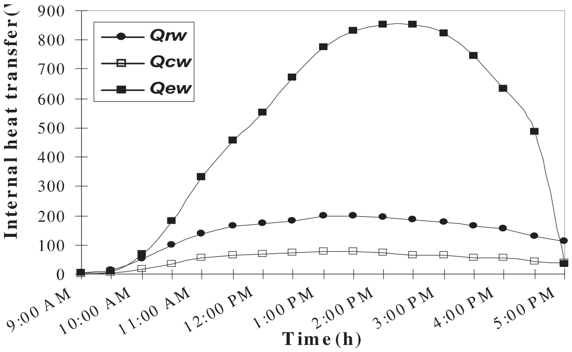

Fig. 8. Variation of internal heat transfer for with charcoal performance

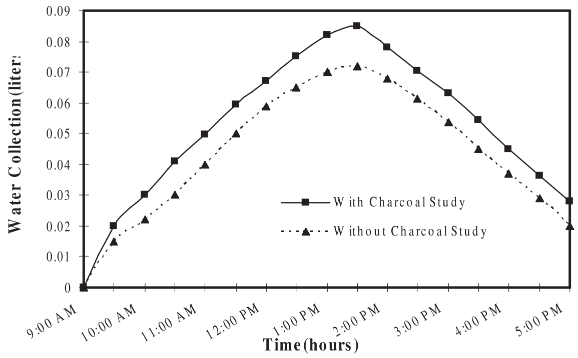

Fig. 9. Variation of water collection with respect to time

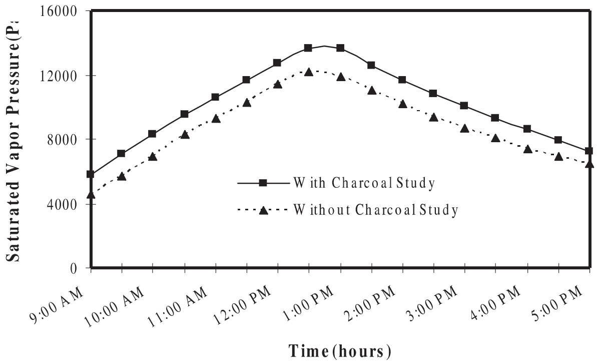

Fig.10. Variation of saturated vapor pressure with respect to time

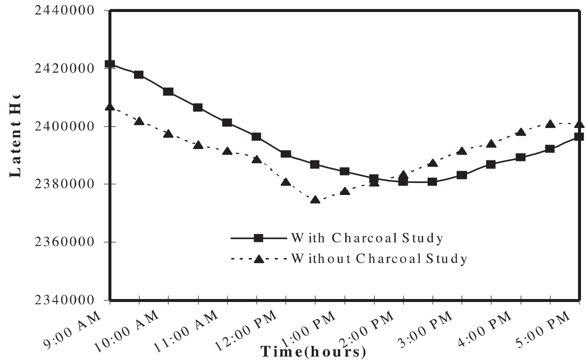

Fig.11. Variation of Latent heat with respect to time

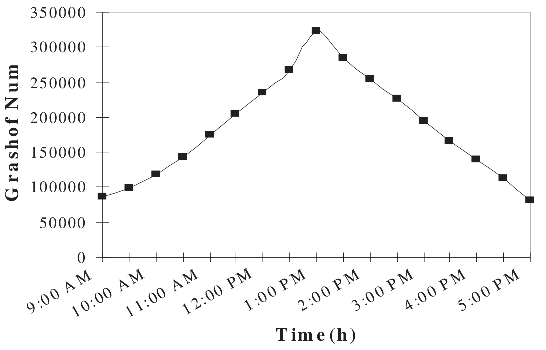

Fig.12. Variation of Grashof Number (charcoal absorber) with respect to time

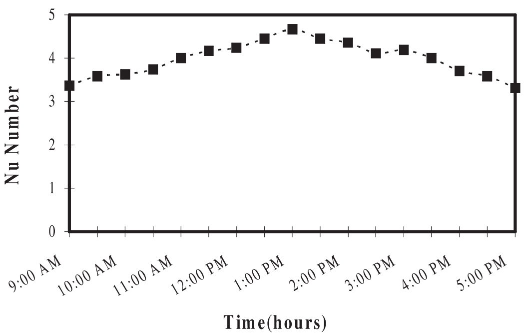

Fig.13. Variation of Nusselt Number (charcoal absorber) with respect to time

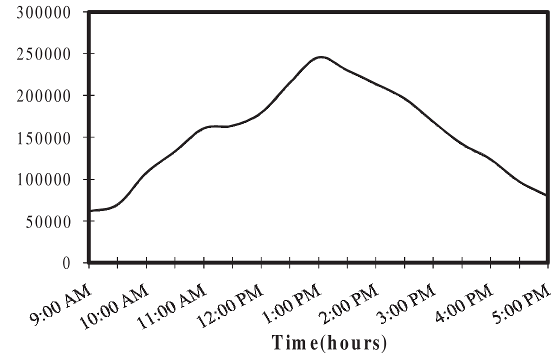

Fig.14. Variation of Grashof Number (without charcoal absorber) with respect to time

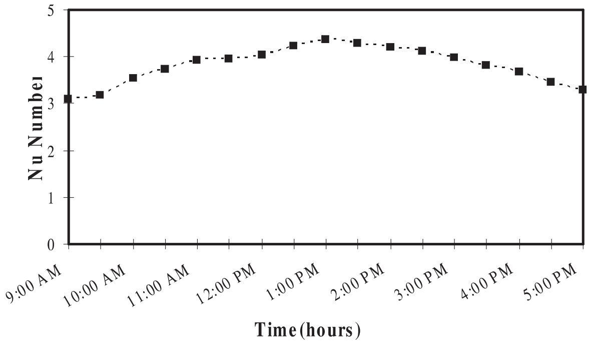

Fig.15. Variation of Nusselt Number (without charcoal absorber) with respect to time

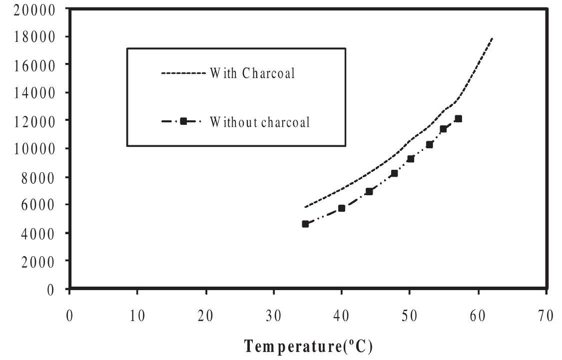

Fig.16. Variation of saturated pressure with respect to temperature

The equation may be modified by

$$Nu_f = 2 + 0.43(Gr_f \Pr_f)^{\frac{1}{4}} \qquad (10)$$

Where

$$Gr = \frac{gb'r^2X^3\Delta T}{J^2}$$

$$\beta' = \frac{1}{\left(T_f + 273\right)}$$

$$X = \frac{A}{P}$$

$$T_f = \frac{(T_1 + T_2)}{2}$$

RESULTS AND DISCUSSION

This type of still receives radiation that is transmitted from the spherical transparent surface. At the same time the water vapor is condensed in the larger spherical surface area. Hence more water droplets are condensed on the surface. The contact in the spherical surface still with air is more than a single slope solar still. Hence the rate of condensed distillate yield is increased. This still has added advantage in evaporating the water by floating the charcoal for absorption of radiation. The performance of spherical solar still was studied with two modes of operation, first spherical solar still with charcoal absorber and then without charcoal absorber. Fig. 3 shows the variation of solar radiation with respect to time in both studies. The solar radiation starts to increase in the morning and attains maximum at the noon and tends to decrease in the evening time. The variation of solar radiation received was in the range of 458.86 W/m^2 to 1086.00 W/m^2 on normal sky days, when still performance was measured with the charcoal absorber. On the other hand, when the still is studied without charcoal absorber, the radiation received was in the range of 507.23 W/m^2 to 1092.00 W/m^2. The average solar radiation received for the spherical solar still with charcoal absorber was 835.24 W/m^2 while the average radiation for without charcoal absorber is 841.27 W/m^2. Figs. 4-5 show the variation of temperature with respect to time for these two experiments. The rise in water temperature ranged from 39°C to 62°C for water temperature 32°C to 60°C for air temperature, 29.5°C to 35.5°C for room temperature, 33 to 38°C for outer cover temperature and 31.9°C to 36°C for ambient air temperature without charcoal absorber. Similarly the rise in water temperature ranged from 40°C to 68°C, 38°C to 62°C for air temperature, 29.5°C to 37°C for room temperature, 33 to 37°C for outer cover temperature and 33°C to 41°C for ambient temperature in spherical solar with charcoal absorber. These temperature variations in this study show that temperature of the still with charcoal absorber was more than the normal still without charcoal absorber, since the charcoal absorbs more radiation and it increases the water temperature to a higher value. Fig. 6 shows the variation of efficiency with respect to time in both studies. The maximum efficiency was observed as 18 % for normal still and 25.34 % for charcoal absorber still. The heat transfer in solar radiation can occur in two modes i.e. external and internal heat transfer. The external heat transfer is governed by conduction, convection and radiation processes, which are independent of each other. This heat transfer occurs outside of the solar distiller from the cover, bottom and side insulation. The heat transfer within the solar distiller is referred to as internal heat transfer mode, which consists of convection, evaporation and radiation. The convective heat transfer occurs simultaneously with evaporative heat transfer and these two heat transfers are independent of radiative heat transfer. The evaporative heat transfer was calculated to be in the range of 11.52 W/m^2 to 645.81 W/m^2, the radiative heat transfer to be in the range of 11.10 W/m^2 to 136.60 W/m^2 and the convective heat transfer to be in the order of 0.87 W/m^2 to 46.21 W/m^2 for this solar still Fig. 7. Fig. 8 shows the internal heat transfer coefficients for with charcoal performance with respect to time. The evaporative heat transfer was calculated to be in the range of 2.90 W/m^2 to 854 W/m^2, the radiative heat transfer to be in the range of 5.36 W/m^2 to 199.56 W/m^2 and the convective heat transfer to be in the order of 0.8773 W/m^2 to 78.51 W/m^2 for spherical solar still with charcoal performance. More evaporative heat transfer coefficient describes the more distillate outputs. These results indicated that the spherical solar still with charcoal absorber is more comfortable for desalination technologies. Fig. 9 shows the variation in water collection with respect to time for both the experiments. The distillates yield was around 2.3 liters/m^2/day without charcoal absorber and 2.8 liters/ m^2/day for with charcoal absorber. Fig. 10 shows the variation of saturated vapor pressure for both the experiments. The calculated saturated vapor pressure is in the range of 4600 Pa to 12187 Pa for normal still and 5800 Pa to 13640 Pa for with absorber. Fig .11 shows the variation of latent heat with respect to time. It was found in the range of 2406949 Kg^{-1} to 2400985 Kg^{-1} without charcoal absorber inside and 2421479 Kg^{-1} to 2396424 Kg $^{-1}$ was observed with charcoal absorber inside the still. Figs. 12-13 show the variations of Grashof number and Nusselt number with respect to time for spherical with charcoal absorber. It has been concluded that Grashof number and Nusselt number increase with respect to time. Grashof number was found to be 87091 to 322746 and the Nusselt number found to be 3.3 to 4.66 in the charcoal absorber study. Similarly Figs. 14-15 show that the variations of Grashof number and Nusselt number with respect to time for still without charcoal absorber. Grashof number was found as 61476 to 245904 and the Nusselt number found as 3.0 to 4.5 for without the charcoal absorber study. Grashof value was found to increase steadily during warm up period and then started to decrease with respect to decrease in water temperature. After attaining the higher temperature, the Nusselt number value maintains a steady state. Fig .16 shows the variation of saturated vapor pressure (N/m^2) with respect to water temperature. From this graph we can easily assess the saturated vapor pressure values for the water temperatures.

REFERENCES

Al- Hussaini, H. and Smith, L.K. 1995. Enhancing of solar still productivity by vacuum technology. *Energy Conversion Management*, 36: 1047-1055.

Al-Karaghouli, A.A. and Alnaser, W.E. 2004. Experimental comparative study of the performance of single and double basin solar still, *Applied Energy*, 77: 317-325.

Badron, A.A. 2001. Inverted trickle solar still, Effect of heat recovery, *Desalination*. 133:167-173.

Badron, O.O. and Al-Hayek. 2004. The effect of using different designs of solar stills on water desalination, *Desalination*. 169: 121-127.

Cappelletti G.M. 2002. An experimental with plastic solar still, *Desalination*. 142: 221-227.

Duffie, J.A. and Beckman, W.A. 1974. *Solar Energy Thermal Process*, John Wiley and Sons, New York.

El-sebaii, A.A. 2005. Thermal performance of a triple basin solar still, *Desalination*. 174: 23-37.

Kabeel, A. E. 2007. Water production from air using multi shelves solar lass pyramid system, *Renewable Energy*. 32: 157-72.

Kelogirous, S. 1998. Use of parabolic trough solar energy collector for sea water desalination, *Applied Energy*, 60: 58-88.

Malik, M.A.S., Tiwari, G.N., Kumar, A. and. Sodha, M.S. 1974. *Solar Desalination*. Pergamon Press, New York.

Malik, M.A.S., Tiwari, G.N., Kumar, A. and Sodha, M.S. 1982. *Solar distillation, a predict study of a wide range of solar and optimum design, construction and performance.* Pergamon press, New York.

Rodriguez, L. Grancia. 2004. Desalination by wind power, *Wind Engineering*. 28: 453.

Tiwari, G.N., Singh, S.K. and Bhatnagra, V.P. 1993. Analytical thermal modeling of multi basin solar still, *Energy Conversion and Management*. 34: 1261-1266.

SYMBOLS

A - Area (m^2)

M_w - Mass of Water (kg)

g - Acceleration due to gravity (m/s^2)

V - Wind Speed (m/sec)

T_a - Air temperature (°C)

T_1 - Hot surface temperature (°C)

T_2 - Surrounding air temperature (°C)

T_w - Water temperature (°C)

T_f - Fluid average temperature (°C)

P - Perimeter of the surface

T_{amb} - Ambient temperature (°C)

T_{sky} - Sky temperature (°C)

T_c - Top Cover Temperature (°C)

C_{pa} - Specific Heat of Air at Constant Pressure (J/Kg °C)

Nu - Nusselt number

Pr - Prandlt number

X - Dimension of the system

ΔT - Temperature difference (°C)

H_s - Incident Solar Radiation on Top Cover per unit area per unit time (W/m^2)

P_a - Partial pressure of water vapor at atmospheric temperature (pa)

P_c - Partial pressure of water vapor at polythene temperature (pa)

P_w - Partial pressure of water vapor at water temperature (pa)

P - Saturated Vapor Pressure (pa)

h_{cw} - Convective Heat Transfer Coefficient from Top Cover to Ambient (W/m^2 °C)

h_{ew} - Evaporative Heat Transfer Coefficient from Water to Top Cover (W/m^2°C)

h_{rw} - Radiation Heat Transfer Coefficient from Top Cover to Ambient (W/m^2 °C)

Q_{cw} - Convective from Water Surface to Top Cover Surface (W/m^2)

Q_{ew} - Evaporation from the Water Surface to the Top Cover (W/m^2)

Q_{rw} - Radiation from the Water Surface to the Top Cover (W/m^2)

Q_{ca} - Heat Transferred from Top Cover to Atmosphere by Convection (W/m^2)

Q_{ra} - External Radiative Heat Transfer from Top Cover (W/m^2)

Q_b - Conduction Heat Transfer through Base (W/m^2)

Q_a - Total Heat Transferred per unit area per unit time from Top Cover to Ambient (W/m^2)

h_i - Heat Transfer Coefficient from Bottom of the Still to the Ambient (W/m^2 ^{o}C)

k - Thermal conductivity

Greek

$\varepsilon_{tc,}$ ε_w ε_{ch} - Emissivity of Top Cover, Water, charcoal respectively

β - Thermal expansion coefficient

η - Efficiency of still (%)

ρ - Partial mass density of water vapor (Kg/m^3)

£ - Latent Heat (^{o}C)

σ - Stefan-Boltzmann constant (5.6697×10^{-8} W/m^{2o}K^4)

τ - Glass absorptive

μ - Dynamic viscosity of the fluid, Pa.s